The spectrum of vibration modes in soft opals

W. Cheng, J. J. Wang, U. Jonas, and W. Steffen
Max Planck Institute for Polymer Research, P.O. Box 3148, 55128 Mainz, Germany

G. Fytas[a)]
Max Planck Institute for Polymer Research, P.O. Box 3148, 55128 Mainz, Germany, Foundation for Research and Technology-Hellas (FORTH)/Institute of Electronic Structure and Laser and Technology, P.O. Box 1527, 71110 Heraklion, Greece, and Department of Materials Science and Technology, University of Crete, 71003 Heraklion, Greece

R. S. Penciu
Foundation for Research and Technology-Hellas (FORTH)/Institute of Electronic Structure and Laser and Technology, P.O. Box 1527, 71110 Heraklion, Greece

E. N. Economou
Foundation for Research and Technology-Hellas (FORTH)/Institute of Electronic Structure and Laser and Technology, P.O. Box 1527, 71110 Heraklion, Greece and Department of Physics, University of Crete, 71003 Heraklion, Greece

(Received 6 June 2005; accepted 2 August 2005; published online 29 September 2005)

Numerous vibrational modes of spherical submicrometer particles in fabricated soft opals are experimentally detected by Brillouin light scattering and theoretically identified by their spherical harmonics by means of single-phonon scattering-cross-section calculations. The particle size polydispersity is reflected in the line shape of the low-frequency modes, whereas lattice vibrations are probably responsible for the observed overdamped transverse mode. © *2005 American Institute of Physics*. [DOI: 10.1063/1.2046607]

The propagation of elastic waves in condensed matter is of long-standing interest in solid-state physics. The discovery of photonic crystals with their particular optical properties has cross-fertilized and further boosted the interest on phononic materials with acoustic pseudogaps and complete gaps at certain frequency ranges. The phenomenon is rich due to the number of parameters of the composite material, i.e., density $\rho(r)$ and the two Lamé coefficients $\lambda(r)$ and $\mu(r)$ which vary periodically in space.[1] The phononic crystals fabricated either by self-assembly,[2] lithographic patterning,[3] or manual construction[4] are characterized by the dispersion $\omega(k)$ relations. At low frequencies, ultrasonic transmission[4] and stimulated Brillouin scattering[5] techniques can be applied with an external generation of the acoustic waves. At hypersonic frequencies, the powerful nondestructive and noncontact Brillouin light-scattering technique utilizes the thermal acoustic phonons propagating in microstructures with spacing d. Given the range of the scattering wave vector q, Brillouin spectroscopy (BS) measures acoustic excitations at hypersonic (GHz) frequencies whose propagation can be a sensitive index of the structure, morphology, and micromechanics of the composite material when $qd=O(1)$.

In colloidal crystals, BS has revealed the presence of various excitations related to particle eigenmodes,[6,7] "Bragg" modes, and mixed modes[7] due to acoustic phonons/particle eigenmodes hybridization. The former are rather weak due to the immediate contact with the fluid medium[8] and hence leakage of the elastic energy. Very recently,[9] the application of BS to a synthetic opal consisting of closely packed SiO_2 (in air) has resolved up to six particle eigenfrequencies describing its spheroidal (i,l) modes where i designates the ith mode of the lth harmonic. The amplitude of the modes decreases monotonically with increasing l for the highly incompressible SiO_2 and hence still many modes are probably missing. Soft synthetic opals recently prepared[10] for a range of particle diameters offer the possibility to enhance the amplitude of the elastic excitations and hence resolve a large number of eigenfrequencies allowing for a rigorous comparison with theoretical calculations.

In this Letter, we have used the recently developed method to fabricate crystalline films of monodisperse polystyrene (PS) spheres in air and measured up to 21 vibrational modes by high-resolution inelastic light (Brillouin) scattering. For five different particle diameters (d) between 170 and 860 nm, this rich experimental spectrum is well captured theoretically proving the scaling relation $\omega(i,l)\sim d^{-1}$ for all localized PS modes with two material elastic constants and the particle size polydispersity. The experiments have revealed an additional unexpected low-frequency continuum mode, which probably relates to overdamped shear waves.

Negatively charged PS colloidal particles were synthesized by emulsion polymerization.[10] Several circles of centrifugation and sonification were performed to remove impurities and obtain monodisperse particles. The soft PS opals were fabricated on glass substrates by vertical lifting deposition from the colloidal suspension (0.5%–2.5% w/w) by means of a homemade dipping device.[10] This is based on a step motor with a 0.5-μm half step which enables withdrawing speeds in the range of 1 μm/s to several cm/s. Low-

[a)]Electronic mail: fytas@iesl.forth.gr

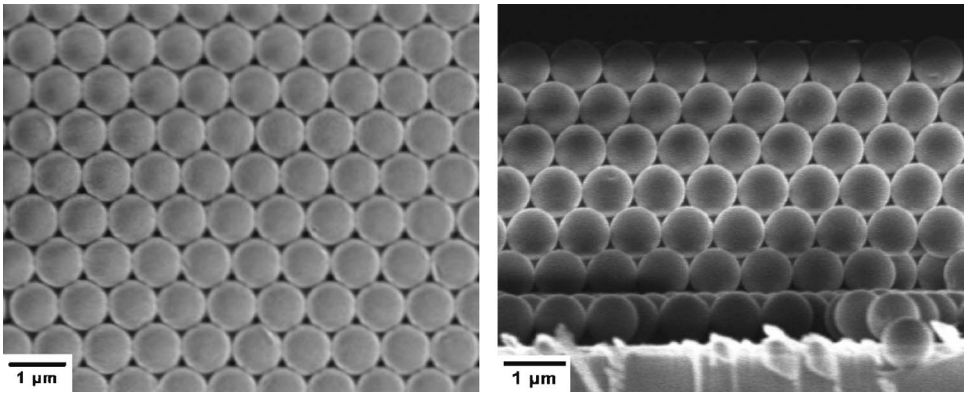

FIG. 1. Scanning electron microscope images (top and side view) of the synthetic opal film consisting of seven ordered layers of monodisperse polystyrene spheres with a diameter of $d=856$ nm.

voltage scanning electron microscope (LV-SEM) images on native samples (nonsputtered) shown for the top and side views in Fig. 1 demonstrate the highly ordered crystalline morphology for seven layers of the monodisperse particles with $d=856\pm15$ nm. Similar crystals were obtained for the five different PS particles with diameters ranging from 170 to 856 nm. The particle diameters for the calculations were obtained from their SEM images.

The PS opals exhibit strong multiple light scattering due to the strong elastic form factor of the individual nanospheres and their large optical contrast with the surrounding air. The scattering wave vector q is therefore ill defined. Hence, the dispersion relations for acousticlike phonons[2,3,6,7] cannot be measured. However, photon multiple scattering was found to enhance the inelastic scattering from localized (q-independent) modes. Figure 2 displays the q-independent Brillouin spectra of the five PS opals recorded at low-scattering (10°) angle by a six-pass tandem Fabry-Perot interferometer.[7] The incident laser beam and the scattered light were both linearly polarized perpendicular to the scattering plane, but due to the scrambling of the polarization the spectra include contributions from longitudinal and transverse modes. For the two largest diameters, the multiple scattering cutoff at about 14 GHz corresponds to the acoustic phonon in bulk PS at $q=4\pi n/\lambda_0$ ($n=1.59$ is the refractive index and $\lambda_0=532$ nm is the laser wavelength) leading to $\lambda\approx5.8$ GPa.

The spectra show several Brillouin doublets with their number and proximity increasing with particle diameter; up to 21 modes are resolved for the highest d in comparison with the six modes observed in silica opals.[9] The q independence of the spectra was verified for the PS opal with the lowest d that exhibits the weakest multiple scattering among all samples and conforms to the localized nature of these modes. Their frequencies in Fig. 2 scale with $1/d$ (Fig. 3). The pertinent features reported, for the first time, in Fig. 2 are (i) the successful scaling of the rich spectrum of the vibration modes, (ii) the line shape and the amplitude of the observed modes, and (iii) the featureless low-frequency spectral component.

We compare the experimental data with the theoretical results obtained by considering a plane sound wave propagating in air and impinging upon a single PS sphere in air. The sphere eigenmodes appear as resonance peaks in the acoustic wave scattering-cross-section plot versus frequency. They depend on the mass density and the speed of sound in air and in the PS particle, as well as on the size of the particle. To reveal more clearly the resonances, we have subtracted from the calculated scattering amplitude the scatter-

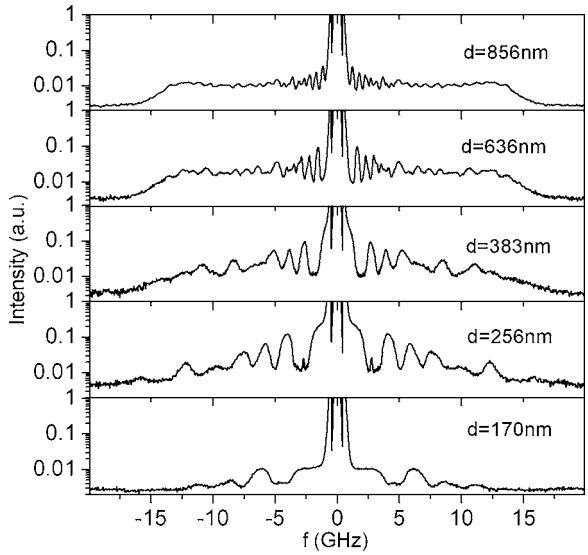

FIG. 2. Brillouin light-scattering spectra of polystyrene opals with five different particle diameters d as indicated in the plot. More than twenty modes can be resolved in the opal with the highest d.

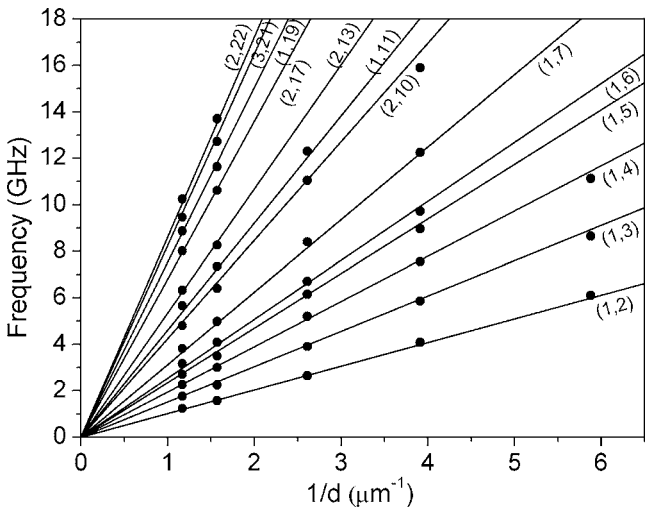

FIG. 3. Peak frequencies of the Brillouin spectra as a function of the inverse diameter. Up to thirteen frequencies are shown to obey the $f\sim d^{-1}$ scaling (solid lines). The numbers (i,l) denote the ith mode of the lth harmonic.

TABLE I. Vibration modes of polystyrene spheres in air.

	$f(i,l)d$ (nm GHz)[a]	$f(i,l)d$ (nm GHz)[b]	(i,l)
1	1040	1017	1,2
2	1480	1518	1,3
3	1900	1945	1,4
4	2310	2348	1,5
5	2480	2538	1,6
6	3140	3119	1,7
7	4100	4237	2,10
8	4700	4607	1,11
9	5290	5340	2,13
10	6780	6797	2,17
11	7450	7523	1,19
12	8100	8247	3,21
13	8730	8609	2,22

[a]Experimental.
[b]Computed.

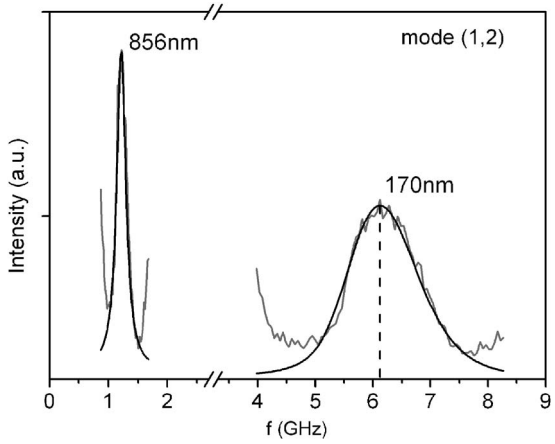

FIG. 4. The lowest-frequency (1,2) mode for the smallest and largest PS spheres represented by Eq. (1) and variance 14 and 10, respectively. For the smallest PS spheres, the vertical dashed line makes the asymmetry of the peak more apparent.

ing amplitude for a rigid sphere of equal size. The peaks in the scattering cross section are very narrow, since the elastic constant and mass density contrast between the PS sphere and the surrounding air is very large and the coupling of the sphere eigenmodes to the surrounding air is small. To avoid the possibility of losing a peak in the calculations (due to its almost δ-function shape) we artificially use instead of the air mass density a larger mass density of 50 $\mathrm{kg/m^3}$, for the matrix material surrounding the particles. This results in a broader width for the calculated peaks without altering their position.

The resonances at frequencies $f(i,l)$ are labeled by (i,l) where l denotes the angular momentum quantum number and i is the order of the mode for a given l. The identification of the quantum numbers in the theory is done by taking the incident sound wave of only one l each time. In our calculations, we used the experimentally provided values for the longitudinal sound velocity $c_L=2350$ m/s and mass density $\rho=1050$ $\mathrm{kg/m^3}$ of PS, while the value of the transverse sound velocity $c_T=1210$ m/s in PS was obtained by fitting the calculated frequencies to the experimental ones. These theoretical calculations with a single adjustable parameter describe the experimental vibration eigenfrequencies very well as demonstrated by the solid lines in Fig. 3 and the comparison between the theoretical and experimental reduced frequencies $f(i,l)d$ in the first and second columns of Table I. The observed agreement allows for the assignment of the observed modes identified by the integers (i,l) which are compiled in Table I. We note here that the sound scattering-cross-section calculations can be used as a method for the determination of unknown material parameters.

For an isolated particle without internal losses, there is no dissipation of the elastic energy which should lead to very narrow spectra indistinguishable from the instrumental function. The observed broad and asymmetric line shape of the experimental peaks, in particular for the low l modes (Fig. 2), is attributed to the finite particle size polydispersity. We theoretically represent this frequency dependence by a convolution of a Gaussian distribution function of the particle size and a Lorentzian line,

$$I(\omega) \approx \int dx A(x) \frac{\Gamma(x)}{(\omega-\omega(x))^2+\Gamma(x)^2} \frac{\exp[-(x-D)^2/2\sigma^2]}{\sqrt{2\pi}\sigma}, \tag{1}$$

where $A(x)\approx A_0$, $\omega(x)=2\pi c_1/x$ is the peak frequency and the natural half-width at half maximum $\Gamma(x)$ is close to the instrumental width for monodisperse particles without internal losses. The experimental spectrum for the lowest-frequency mode (1,2) of the smallest (170 nm) and largest (856 nm) PS spheres can be reproduced well (solid lines in Fig. 4) by Eq. (1) by using fixed $c_1=1020$ nm GHz (the slope of the solid line in Fig. 3) and the variance σ as the only adjustable parameter besides the amplitude A_0. The different shape of the experimental spectrum of the (1,2) mode for these two diameters is partly due to the $\omega\sim 1/d$ dependence and the different size polydispersity ($\sigma=14$ and 10) with the large particle possessing lower σ. The obtained values of the variance conform to the size distribution extracted from the SEM images. For particles in nanometer and micrometer ranges, the eigenfrequencies fall in the teraherz[11] and megahertz[12] ranges, respectively.

The detailed mechanism for the formation of ordered colloidal films by vertical deposition is still not fully understood.[10] There should be, however, a coupling between adjacent spheres originating from capillary neck-based restoring forces owing to the presence of a thin water film between the particles and some polar and chargeable groups on the surface of the particles.[10] These forces are thought to cause viscoelastic shear response and can be probably responsible for the central overdamped mode in the spectra of Fig. 2.

Following a treatment by Landau and Lifshitz,[13] the viscous force F on each sphere is $F\approx-\eta v A/x$ where A denotes the sphere-water contact area, x is the characteristic length of the variation of the transverse wave, $v=\omega y$ is the velocity of the transverse wave, y is its amplitude, ω is its angular frequency, and η is the viscosity of the thin water layer with a density ρ. In the present case, the length x is assumed to be the surface to surface distance of adjacent spheres. The total

losses ΔE per period is of the order of $NFy\omega = \eta\omega^2 y^2 AN/x$ where N is the number of particles. On the other hand, the kinetic energy E_k of the transverse wave is of the order of $V\rho\omega^2 y^2$ where $V = NV_0/\phi$, V_0 is the volume of the sphere, and ϕ is the volume fraction. The relative energy dissipation for this transverse wave, $\Delta E/E_k \sim (\eta/\rho)A/(V_0 x\omega)$ can be $O(1)$ for the kinematic viscosity of water, $\eta/\rho = 0.01$ cm^2/s, $A/V_0 \sim 1/d^{(1+\nu)}$, and $x \sim 10$ nm where it was assumed that $A/d^2 \sim 1/d^\nu$ accounts for the expected increased percentage of sphere-water contact as d decreases. Hence, this mode is overdamped and its width, $\Gamma_0 \approx (\eta/\rho)A/(V_0 x)$ should scale with $d^{-(1+\nu)}$. On the experimental side, the cutoff frequency of the low-frequency component for the PS opals with the three lower diameters in Fig. 2 conforms to $\nu = 0.3$. Based on this qualitative trend, the high-frequency modulus of the lattice[14] $G_\infty = k/d$ with $k \sim \Gamma_0 \eta d$ being the spring constant of the interaction between a pair of spheres is estimated to be of the order of GPa, i.e., an order of magnitude larger than for colloidal crystal suspensions.[14]

In this Letter, we demonstrate that high-resolution Brillouin spectroscopy can reveal a large number of vibration eigenmodes of submicrometer particles in synthetic soft opals. All these hypersonic frequencies are identified by spherical harmonics $Y_{lm}(\theta, \varphi)$ angular dependence and the radial $R_l(r)$ variation in analogy to the atomic orbitals. The peculiar line shape of the low-frequency modes is a sensitive index of the particle size distribution. The presence of thin water films between adjacent particles and some chargeable polar groups may account for both a relatively large shear modulus and a low-frequency overdamped mode. As colloidal particle crystals are considered for an increasing number of potential applications in photonics for optical signal and data processing and sensor applications, the establishment of a nondestructive high-resolution optical technique opens new means for micromechanical characterization in phononic and photonic structures in the spectral region of visible light.

We thank MPG and EC (SoftComp NoE) for the financial support.

[1] M. Sigalas, and E. N. Economou, J. Sound Vib. **158**, 377 (1992); see also I. E. Psarobas, A. Modinos, R. Sainidou, and N. Stefanou, Phys. Rev. B **65**, 064307 (2002), and references therein.
[2] A. Urbas, E. L. Thomas, H. Kriegs, G. Fytas, R. S. Penciu, and E. N. Economou, Phys. Rev. Lett. **90**, 108302 (2003).
[3] T. Gorishnyy, C. K. Ullal, M. Maldovan, G. Fytas, and E. L. Thomas, Phys. Rev. Lett. **94**, 115501 (2005).
[4] Z. Liu, X. Zhang, Y. Mao, Y. Y. Zhu, Z. Yang, C. T. Chan, and P. Sheng, Science **289**, 1734 (2000).
[5] L. Dhar and J. A. Rogers, Appl. Phys. Lett. **77**, 1402 (2000).
[6] J. Liu, L. Ye, D. A. Y. Weitz, and P. Sheng, Phys. Rev. Lett. **65**, 2602 (1990).
[7] R. S. Penciu, H. Kriegs, G. Petekidis, G. Fytas, and E. N. Economou, J. Chem. Phys. **118**, 5224 (2003).
[8] L. Saviot and D. B. Murray, Phys. Rev. Lett. **93**, 217801 (2004).
[9] M. H. Kuok *et al.*, Phys. Rev. Lett. **90**, 255502 (2003); **91**, 149901(E) (2003).
[10] G. T. D. Shouldice *et al.*, Eur. Polym. J. **30**, 179 (1994); C. Krueger and U. Jonas, J. Colloid Interface Sci. **252**, 331 (2002); U. Jonas and C. Krueger, J. Supramol. Chem. **2**, 255 (2002).
[11] E. Duval, A. Bourkenter, and R. Shampagnon, Phys. Rev. Lett. **56**, 2052 (1986); M. Ikezawa, T. Okuno, and Y. Masumoto, Phys. Rev. B **64**, 201315 (2001).
[12] M. de Billy, J. Acoust. Soc. Am. **110**, 710 (2001).
[13] L. D. Landau and E. M. Lifshitz, *Fluid Mechanics* (Pergamon, London, 1959), p. 94.
[14] Z. Cheng *et al.*, Phys. Rev. Lett. **85**, 1460 (2000); M. Hoppenbrouwers and W. van de Water, *ibid.* **80**, 3871 (1998).